Technical University of Denmark

Distributed Model Predictive Control of A Wind Farm for Optimal Active Power Control

Part II: Implementation with Clustering based
Piece-Wise Affine Wind Turbine Model.

Zhao, Haoran; Wu, Qiuwei; Guo, Qinglai ; Sun, Hongbin; Xue, Yusheng

DTU Library
Technical Information Center of Denmark

Distributed Model Predictive Control of A Wind Farm for Optimal Active Power Control
Part II: Implementation with Clustering based Piece-Wise Affine Wind Turbine Model

Haoran Zhao, *student member, IEEE,* Qiuwei Wu, *member, IEEE*, Qinglai Guo, *senior member, IEEE,*
Hongbin Sun, *senior member, IEEE* and Yusheng Xue, *senior member, IEEE*

Abstract-**This paper presents Distributed Model Predictive Control (D-MPC) of a wind farm for optimal active power control using the fast gradient method via dual decomposition. The objectives of the D-MPC control of the wind farm are power reference tracking from the system operator and wind turbine mechanical load minimization. The optimization of the active power control of the wind farm is distributed to the local wind turbine controllers. The D-MPC developed was implemented using the clustering based piece-wise affine wind turbine model. With the fast gradient method, the convergence rate of the D-MPC has been significantly improved which reduces the iteration numbers. Accordingly, the communication burden is reduced. A wind farm with 10 wind turbines was used as the test system. Case studies were conducted and analyzed which include the operation of the wind farm with the D-MPC under low and high wind conditions, and the dynamic performance with a wind turbine out of service. The robustness of the D-MPC to errors and uncertainties was tested by case studies with consideration of the errors of system parameters.**

Index Terms-**Dual decomposition, distributed model predictive control (D-MPC), fast gradient method, wind farm control.**

I. INTRODUCTION

W IND energy has become the fastest developing renewable energy and is widely utilized in power systems around the world. Accordingly, the scale of the wind farm grows. Nowadays, a large wind farm may consist

of several hundred individual wind turbines and cover extended area of hundreds of square miles. For example, the largest onshore wind farm under construction, the Gansu Wind Farm in China, has a capacity of over 5,000 MW with a goal of 20,000 MW by 2020.

Wind farms are required to meet more stringent technical requirements for better controllability specified by system operators [1]-[3]. The requirements specify different types of power control: absolute power limitation, delta limitation, balance control, stop control, ramp limitation and fast down regulation to support the system operation and control [4]. To fulfill these requirements, a wind farm shall be capable of tracking specific power references. In other words, the modern wind farm is required to operate much more like a conventional power plant and ultimately to replace conventional power plants.

The control scheme of a wind farm to support the system wide control can be implemented either by utilization of a separate energy storage device or through derated operation of wind turbines [5]. However, with the increasing scale of wind farms, the additional capital investment and maintenance cost of the energy storage system would be too high. The coordination of the wind turbine control is a more practical solution. Since the wind farm is required to produce less than the maximum available power, the wind turbines will limit their power production. This implies that they can vary their power production in response to wind speed fluctuations as long as the total power production of the farm meets the demand.

In [4], the dispatch function of each turbine is based on the available power. In [5], the additional power references are proposed to spread over all the turbines proportionally to their actual output power. The work above focuses only on tracking the power reference. The wind turbine mechanical load (load for short hereinafter), referring to the forces and moments experienced by the wind turbine structure, is not included. This will significantly shorten the service lifetime of wind turbines [6].

Recently, the wind farm control with the load optimization has been studied in several references [7]-[10]. The control objective is to dynamically redistribute power in order to minimize the loads experienced by the turbines while maintaining the desired power production at all times [8]. A Linear Quadratic Gaussian (LQG) controller was introduced in [7], [8]. The computation burden is distributed via gradient descent method which relies only on a few measurements.

H. Zhao is with Center for Electric Power and Energy, Department of Electrical Engineering, Technical University of Denmark, Kgs. Lyngby, 2800, Denmark, and Sino-Danish Center for Education and Research, Aarhus, 8000 Denmark (email: hzhao@elektro.dtu.dk).

Q. Wu is with Center for Electric Power and Energy, Department of Electrical Engineering, Technical University of Denmark, Kgs. Lyngby, 2800, Denmark, and Sino-Danish Center for Education and Research, Aarhus, 8000 Denmark, and State Key Lab. of Power System, Dept. of Electrical Engineering, Tsinghua University, Beijing 100084, China (email: qw@elektro.dtu.dk).

Q. Guo and H. Sun are with Department of Electrical Engineering, Tsinghua University, Beijing 100084, China (email: guoqinglai@tsinghua.edu.cn, shb@mail.tsinghua.edu.cn).

Y. Xue is with State Grid Electric Power Research Institute, Nanjing, 210003, China (e-mail: xueyusheng@sgepri.sgcc.com.cn).

The Model Predictive Control (MPC) scheme based on multi-objective performance optimization is another effective solution to handle this problem. It makes use of the receding horizon principle such that a finite-horizon optimal control problem is solved over a fixed interval of time [11]. The main advantage of the MPC compared to the LQG control is that the MPC can realize control with input and output constraints. The centralized MPC (C-MPC) algorithm has been developed for wind farm control in [9], [10]. The optimal power set-points are explicitly computed offline by multi-parametric programming for each turbine. These set points are based on other auxiliary power variables and are then used for online coordination of the turbines in order to meet the total power demand. However, the wind farm model is described as a coupled, constrained multiple-input and multiple output (MIMO) system whose order drastically grows with the increasing number of wind turbines. The computation burden of the C-MPC makes it impractical for real-time application.

The Distributed MPC (D-MPC) concept is developed to solve the same optimization problems as the C-MPC with much reduced computation. Each wind turbine can be considered as a single distributed unit. These units are coupled by the shared wind field and the power demand to the wind farm. Among the different distributed algorithms ([12], [13]), some are based on the property that the (sub)gradient to the dual of optimization problems can be handled in a distributed manner [14]. This approach is referred as the dual decomposition. The fast gradient method used in the dual decomposition has attracted more and more attention for the D-MPC in the past few years [15]-[18]. Compared with the standard gradient methods, the convergence rate can be largely improved.

The main contribution of this paper is the D-MPC design for the wind farm control which strikes a balance between the power reference tracking and the minimization of the wind turbine loads. The parallel generalized fast dual gradient method is adopted. This control structure is independent from the scale of the wind farm and the communication burden between local D-MPC and the central unit is largely reduced.

The paper is organized as follows: Section II describes the wind farm controller based on the D-MPC. The wind turbine load is evaluated in Section III. Section IV explains the design of the D-MPC for a wind farm. Case studies with the developed D-MPC are presented and discussed in Section IV followed by conclusions.

II. WIND FARM CONTROL BASED ON D-MPC

The wind speed can be considered as a mean value with turbulent fluctuations superimposed. Consequently, the wind field dynamics can be represented by two decoupled time scales [9], [19]. The slow dynamic related to the mean wind speed is used to represent the propagation of wind stream traveling through the wind farm. Due to the wake effects, there is coherence between wind turbines. According to the wind field model and measurements of the wind farm, the mean wind speed of individual wind turbine can be estimated. The fast time scale dynamic related to the wind turbulence and gusts. The turbulence of different wind turbines is considered uncoupled which results in the load increase.

The hierarchical structure of the D-MPC active power control of a wind farm is illustrated in Fig. 1. Similar to the hierarchical structure proposed in [10], the high level control operates at a slow time scale. Specifically, the wind farm power reference $P_{\mathrm{ref}}^{\mathrm{wfc}}$ is generated based on the requirements from the system operator and the available wind farm power. With the wind field model and measurement data, the mean wind speed of a certain period (several minutes) can be estimated. Several approaches have been developed to distribute the mean power references to individual wind turbines ($\overline{P_{\mathrm{ref}}^{\mathrm{WT_1}}}$, $\overline{P_{\mathrm{ref}}^{\mathrm{WT_2}}}$, $\cdots$, $\overline{P_{\mathrm{ref}}^{\mathrm{WT_i}}}$) with $\sum \overline{P_{\mathrm{ref}}^{\mathrm{WT_i}}} = P_{\mathrm{ref}}^{\mathrm{wfc}}$, which is reviewed in [10]. The proportional distribution algorithm proposed in [4] is adopted to distribute the mean power references to individual wind turbines which are according to the available power of each turbine.
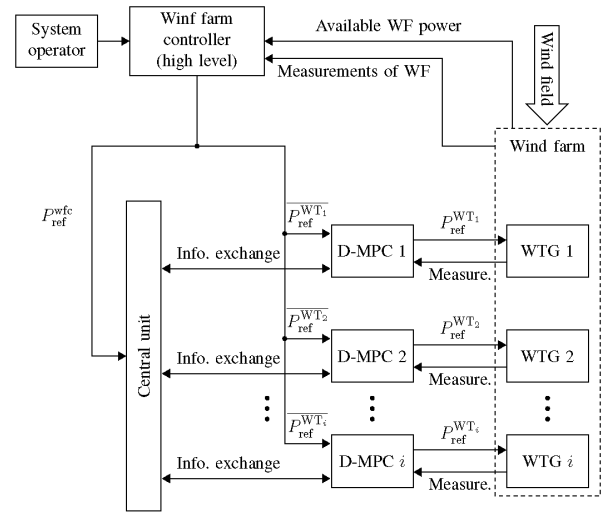

Fig. 1 Control structure of the active power control of a wind farm based on D-MPC

Conventionally, these mean power reference signals are directly assigned to the individual wind turbines without considering the effect of turbulence. In this paper, these references are modified by the D-MPC controller locally equipped at each wind turbine, which can be considered as the low level wind farm control for short time scale dynamics. It can reduce the wind turbine load by adjusting the power reference to each turbine.

By using the clustering based piece-wise affine wind turbine model developed in Part I and the measurement feedback, the D-MPC can determine in which operation region the wind turbine is. The corresponding prediction model and the matrix for local optimization can be formulated. With the communication with the central unit (see Fig. 1), the iterations are executed to meet the global constraints. Different from [9] and [10], the central unit doesn't have much computation. It is used to update the dual variables by collecting the matrices from wind turbines which are computed off-line. More details are described in Section IV. Then the modified power references ($P_{\mathrm{ref}}^{\mathrm{WT_1}}$, $P_{\mathrm{ref}}^{\mathrm{WT_2}}$, $\cdots$, $P_{\mathrm{ref}}^{\mathrm{WT_i}}$) with $\sum P_{\mathrm{ref}}^{\mathrm{WT_i}} = P_{\mathrm{ref}}^{\mathrm{wfc}}$ are assigned to the individual wind

turbine controller. The reference signals for the converters and blade pitch controller of each wind turbine are generated according to $P_{\mathrm{ref}}^{\mathrm{WT}_i}$.

III. WIND TURBINE LOAD EVALUATION

The additional objective of the D-MPC wind farm control is minimizing the loads of the wind turbines. In this paper, the term load mainly focuses on the load of the tower structure due to the tower deflection and the load on the gearbox due to the torsion of the shaft. Compared with the static loads, the dynamic stress causing the structural damage of the wind turbine is considered to be a much bigger issue [9].

For the tower structure, the wind turbine tower is excited by the thrust force $F_{\mathrm{t}}^{\mathrm{WT}_i}$ caused by the wind flowing on the rotor. The oscillatory transient leads to an undesired nodding of the tower, causing fatigue of the wind turbine tower. Additionally, the relative wind speed is affected as the turbine moves. For the gearbox, the torsional shaft torque $T_{\mathrm{s}}^{\mathrm{WT}_i}$ is transmitted through gearbox. Since it is a vulnerable part, the oscillatory transient of $T_{\mathrm{s}}^{\mathrm{WT}_i}$ causes micro cracks in the material which can further lead to the component failure.

A quadratic load description of a single wind turbine is proposed in [9], [10],

$$\| T_{\mathrm{s}}^{\mathrm{WT}_i}(t) - \overline{T_{\mathrm{s}}^{\mathrm{WT}_i}} \|^2_{Q_T} + \| \frac{dF_{\mathrm{t}}^{\mathrm{WT}_i}(t)}{dt} \|^2_{Q_F} \quad (1)$$

where $\overline{T_{\mathrm{s}}^{\mathrm{WT}_i}}$ indicate the torsional torque at steady state, Q_T and Q_F are the weighting factors. It could be further used to formulate a quadratic cost function for the D-MPC design, which is described in Section IV.

IV. D-MPC THROUGH DUAL DECOMPOSITION WITH FAST DUAL GRADIENT METHOD

A. Wind turbine linearization for D-MPC

The discrete model of a single wind turbine developed in Part I is used as the prediction model. It is a Piece-Wise Affine (PWA) model whose operation regions are determined according to the current state and input variables $[\omega_{\mathrm{r}}, v_{\mathrm{w}}, \theta, P_{\mathrm{ref}}^{\mathrm{WT}}]'$. Accordingly, the computation task of the prediction model has been done offline and stored based on these regions. Since these states can be directly measured and wind speed can be well estimated, the prediction model can be updated by searching the current operation region for each time step. It should be noticed that wind speed in this paper refers to "Effective wind speed" which is used to describe the wind speed affecting the entire rotor. The estimation methods have been nicely reviewed and compared in [20]. For the D-MPC design in this paper, it is necessary to obtain a discrete Linear Time-Invariant (LTI) wind turbine model. Therefore, it is assumed that the obtained prediction model is kept invariant during the prediction horizon, expressed by,

$$\begin{aligned} x(k+1) &= A_{\mathrm{d}}x(k) + B_{\mathrm{d}}u(k) + E_{\mathrm{d}}d(k) + F_{\mathrm{d}} \\ y(k) &= C_{\mathrm{d}}x(k) + D_{\mathrm{d}}u(k) + G_{\mathrm{d}}d(k) + H_{\mathrm{d}} \end{aligned} \quad (2)$$

where x, u, d and y indicate state, input, disturbance and output vectors, respectively: $x = [\omega_{\mathrm{r}}, \omega_{\mathrm{f}}, \theta]'$, $u = P_{\mathrm{ref}}^{\mathrm{WT}}$, $d = v_{\mathrm{w}}$, $y = [T_{\mathrm{s}}, F_{\mathrm{t}}]'$, θ is the pitch angle, ω_{r} and ω_{f} are the rotor speed and the filtered generator speed, respectively, F_{t} is the thrust force, T_{s} is the shaft torque, $P_{\mathrm{ref}}^{\mathrm{WT}}$ is reference power derived from the wind farm, v_{w} represents the wind speed, which is regarded as a disturbance. The formulation of A_{d}, B_{d}, C_{d}, D_{d}, E_{d}, F_{d}, G_{d} and H_{d} depending on the sampling time is explained in Part I.

B. MPC problem formulation

The cost function of the D-MPC design takes into account both the tracking performance of the wind farm power reference and the minimization of the wind turbine load. During the wind farm operation, it is assumed that the mean wind speed $\overline{v_{\mathrm{w}}}$ of a certain period (10 minutes used in [9]) can be estimated and an initial distribution of individual wind turbine power references for this period is known. Therefore, the mean power reference for the i th wind turbine $\overline{P_{\mathrm{ref}}^{\mathrm{WT}_i}}$ can be calculated by a proportional algorithm according to the available power.

$$\overline{P_{\mathrm{ref}}^{\mathrm{WT}_i}} = \alpha_i P_{\mathrm{ref}}^{\mathrm{wfc}}, \quad \text{with} \sum_{i=1}^{n_{\mathrm{t}}} \alpha_i = 1 \quad (3)$$

where n_{t} is the number of wind turbine in the wind farm, $P_{\mathrm{ref}}^{\mathrm{wfc}}$ is the power reference for the wind farm, α_i indicates the distribution factor for the i th wind turbine. Accordingly, other steady state variables, e.g. the shaft torque $\overline{T_{\mathrm{s}}^{\mathrm{WT}_i}}$, can be determined. The prediction horizon is chosen as n_{p} and k indicates the prediction index. By defining

$$\begin{aligned} P_{\mathrm{g}}^{\mathrm{WT}_i}(k) &= u_i(k), \\ T_{\mathrm{s}}^{\mathrm{WT}_i}(k) &= S_1 \cdot y_i(k), S_1 = [1,0], \\ F_{\mathrm{t}}^{\mathrm{WT}_i}(k) &= S_2 \cdot y_i(k), S_2 = [0,1], \\ u_i &= [u_i(0),...,u_i(n_{\mathrm{p}}-1)]', u_i \in \Box^{n_{\mathrm{p}} \times 1} \\ u &= [u_1',...,u_{n_{\mathrm{t}}}']', u \in \Box^{(n_{\mathrm{p}} \cdot n_{\mathrm{t}}) \times 1} \end{aligned}$$

the MPC problem at time t can be formulated as follows,

$$\begin{aligned} \min_{u} \quad & \sum_{i=1}^{n_{\mathrm{t}}} (\sum_{k=0}^{n_{\mathrm{p}}} \Box u_i(k) - \overline{P_{\mathrm{ref}}^{\mathrm{WT}_i}} \Box^2_{Q_P} \\ + \quad & \sum_{k=0}^{n_{\mathrm{p}}} \Box S_1 \cdot y_i(k) - \overline{T_{\mathrm{s}}^{\mathrm{WT}_i}} \Box^2_{Q_T} \\ + \quad & \sum_{k=0}^{n_{\mathrm{p}}-1} \Box \Delta(S_2 \cdot y_i(k)) \Box^2_{Q_F}) \end{aligned} \quad (4)$$

subject to

$$\begin{aligned} x_i(k+1) &= A_{\mathrm{d}}x_i(k) + B_{\mathrm{d}}u_i(t) + E_{\mathrm{d}}d_i(k) + F_{\mathrm{d}} \\ & i \in [1,...,n_{\mathrm{t}}], k \in [0,...,n_{\mathrm{p}}-1] \end{aligned} \quad (5)$$

$$\begin{aligned} y_i(k) &= C_{\mathrm{d}}x_i(k) + D_{\mathrm{d}}u_i(k) + G_{\mathrm{d}}d_i(k) + H_{\mathrm{d}} \\ & i \in [1,...,n_{\mathrm{t}}], k \in [0,...,n_{\mathrm{p}}] \end{aligned} \quad (6)$$

$$x_i(0) = x_i(t) \tag{7}$$

$$\sum_{i=1}^{n_t} u_i(0) = P_{\text{ref}}^{\text{wfc}} \tag{8}$$

$$x_i \in \mathrm{X}_i, u_i \in \mathrm{U}_i, \tag{9}$$

where Q_P, Q_T and Q_F are the weighting factors. The second and third terms in the cost function (3) are used to penalize the deviation of the shaft torque from the steady state and the derivative of the thrust force in order to reduce the wind turbine load, X_i and U_i are the local state and control input constraint sets, respectively. As the optimization variable u, the first values ($u_i(0), i \in [1,...,N_t]$) are taken as the control inputs for each turbine. The control inputs are coupled whose sum equals to the power reference of the wind farm $P_{\text{ref}}^{\text{wfc}}$ (see (8)).

C. Parallel generalized fast dual gradient method

1) Primal problem: The MPC problem in Section IV. B can be reformulated as a standard Quadratic Programming (QP) problem which is rewritten in the following format with Hessian matrix $H_i \in \square^{\,n_p \times n_p}$ (positive definite) and coefficient vector $g_i \in \square^{\,n_p \times 1}$. H_i and g_i can be calculated according to the equality constraints (5), (6) and prediction horizon n_p. More details are described in [21].

$$\min_u \Phi = \sum_{i=1}^{n_t} \Phi_i(u_i) = \sum_{i=1}^{n_t} (\frac{1}{2} u_i' H_i u_i + g_i' u_i) \tag{10}$$

subject to

$$Gu = b \tag{11}$$

$$u \in \mathrm{U}. \tag{12}$$

In this case, the coupling of the control inputs can be equivalently rewritten as the equality constraint (11). Since only the first control input u_i are coupled with all the others,

$$\sum_{i=1}^{n_t} u_i(0) = P_{\text{ref}}^{\text{wfc}}, G \text{ and } b \text{ can be obtained,}$$

$$G = [G_1,...,G_{n_t}], G_i = [1,0,...,0], G_i \in \square^{\,1 \times n_p}$$

$$b = P_{\text{ref}}^{\text{wfc}}$$

2) Properties of dual problem: In this part, the key properties required to apply fast dual gradient methods are described. Obviously, the functions Φ and Φ_i are strongly convex with matrix H and H_i. H is defined as $H = \text{blkdiag}(H_1,...,H_{n_t})$. By introducing the dual variables λ, the primal problem is transformed into the following Lagrange dual problem,

$$\sup_\lambda \inf_u \{\Phi(u) + \lambda(Gu - b)\}$$
$$= \sup_\lambda \sum_{i=1}^{n_t} [\inf_{u_i} \{\Phi_i(u_i) + (\lambda G_i) u_i\} - \lambda \frac{b}{n_t}]. \tag{13}$$

With the definition of conjugate functions for Φ and Φ_i,

$$\Phi^{\mathring{a}}(-G'\lambda) = \sup_u \left(-\lambda Gu - \Phi(u)\right),$$

$$\Phi_i^{\mathring{a}}(-G_i'\lambda) = \sup_{u_i} \left(-\lambda G_i u_i - \Phi_i(u_i)\right),$$

the dual problem above can be rewritten as,

$$\sup_\lambda \left\{ -\Phi^{\mathring{a}}(-G'\lambda) - \lambda b \right\}$$
$$= \sup_\lambda \sum_{i=1}^{n_t} \left[-\Phi_i^{\mathring{a}}(-G_i'\lambda) - \lambda \frac{b}{n_t} \right]. \tag{14}$$

For simplicity, the following dual problem equations are defined,

$$d_i(\lambda) = -\Phi_i^{\mathring{a}}(-G_i'\lambda) - \lambda \frac{b}{n_t}. \tag{15}$$

$$d(\lambda) = -\Phi^{\mathring{a}}(-G'\lambda) - \lambda b, d = \sum_{i=1}^{n_t} d_i. \tag{16}$$

The following property for the dual problem can be derived according to [17], which is the theoretical foundation for the distribution optimization algorithm. The proof is presented in [17].

Property: If the primal function Φ and its local function Φ_i are strongly convex with matrices H and H_i, we have the conclusion that the dual function d and its local function Φ_i (defined in (16) and (15), respectively) are concave, differentiable and satisfies

$$d(\lambda_1) \geq d(\lambda_2) + \nabla d(\lambda_2)(\lambda_1 - \lambda_2) - \frac{1}{2} \| \lambda_1 - \lambda_2 \|_{\mathbf{L}}^2$$

$$d_i(\lambda_1) \geq d_i(\lambda_2) + \nabla d_i(\lambda_2)(\lambda_1 - \lambda_2) - \frac{1}{2} \| \lambda_1 - \lambda_2 \|_{\mathbf{L}_i}^2 \tag{17}$$

for every λ_1, λ_2, $\mathbf{L}$ with $\mathbf{L} \pm GH^{-1}G'$ and $\mathbf{L}_i$ with $\mathbf{L}_i \pm G_i H_i^{-1} G_i'$.

Compared with what has been presented in the literature, this property provides a tighter quadratic lower bound to the dual function. It can be further proved that the obtained bound is the best obtained bound. Therefore, more accurate approximation of the dual function can be derived, which improves the convergence rate. In the next part, a generalized parallel optimization algorithm for D-MPC proposed in [17] is described.

3) Distributed optimization algorithm The parallel fast dual gradient method is implemented below for the wind farm control. Dual variables λ, η and φ are introduced. Normally, the iteration stops if the stopping criterion is met. In this paper, a fixed number of iteration $k_{\max}$ is selected as the stopping criterion in order to limit the online computation time.

Parallel fast dual gradient method for wind farm control

Require: Initial guesses $\lambda^{[1]} = \eta^{[0]}$, $\varphi^{[1]} = 1$.

For $k = 1,...,k_{\max}$, **do**

1) Send $\lambda^{[k]}$ to all wind turbines $j \in \{1,...,n_t\}$ through communication (Central Unit $\Rightarrow$ D-MPC).

2) Update and solve the local optimization with

augmented cost function in individual D-MPC:

$$u_i^{[k]} = \arg\min_{u_i}\{\Phi_i + u_i' G_i' \lambda^{[k]}\} .$$

3) Update $\mathbf{L}_i^{-1}$ in individual D-MPC, if the operating region changes.

4) Receive $u_i^{[k]}$ from each turbine and form $u^{[k]} = (u_1^{[k]},...,u_{n_t}^{[k]})$ (D-MPC $\Rightarrow$ Central Unit).

5) Receive the updated $\mathbf{L}_i^{-1}$ (D-MPC $\Rightarrow$ Central Unit).

6) Update $\mathbf{L}^{-1}$ according to $\mathbf{L}_i^{-1}$ and the dual variables in Central Unit:

$$\eta^{[k]} = \lambda^{[k]} + \mathbf{L}^{-1}(Gu^{[k]} - b)$$

$$\varphi^{[k+1]} = \frac{1 + \sqrt{1 + 4(\varphi^{[k]})^2}}{2}$$

$$\lambda^{[k+1]} = \eta^{[k]} + (\frac{\varphi^{[k]} - 1}{\varphi^{[k+1]}})(\eta^{[k]} - \eta^{[k-1]})$$

End for

According to the property in (17), the algorithm is proved to converge with the rate,

$$d(\lambda^{\mathring{a}}) - d(\lambda^k) \le \frac{2\| \lambda^{\mathring{a}} - \lambda_2 \|_{\mathbf{L}}^2}{(k+1)^2}, \forall k \ge 1 \tag{18}$$

where k represents the iteration number. The details of the proof are described in [17]. As illustrated, the convergence rate is improved from $\mathrm{O}(1/k)$ to $\mathrm{O}(1/k^2)$ with negligible increase in iteration complexity, compared with the standard gradient method. As proposed in [17], $\mathbf{L} = GH^{-1}G'$ has the tightest lower bounds to $d(\lambda)$ and is adopted in this paper.

Since all the turbines are correlated, the $\mathbf{L}^{-1}$ can be calculated as follows:

$$\mathbf{L}^{-1} = \sum_{i=1}^{n_p} \mathbf{L}_i^{-1} = \sum_{i=1}^{n_p} (G_i H_i^{-1} G_i)^{-1}. \tag{19}$$

To be noticed, the linearized model of the individual turbine varies with the change of the operating region. As described in Section IV.C, H_i is dependent on model parameter. Accordingly, the Hessian matrix H_i is time-variant which further leads to the variation of $\mathbf{L}_i^{-1}$. Obviously, the variables involved in the computation, including H_i and $\mathbf{L}_i^{-1}$, can be pre-computed offline and stored according to the operation regions.

The computation burden of the Central Unit only consists of the calculation of $\mathbf{L}^{-1}$ which is the simple addition of the individual $\mathbf{L}_i^{-1}$ and the dual variable updates during iterations. Most computation tasks are distributed to the local D-MPCs. Besides, due to the reduced iteration number, the communication burden between D-MPC and the Central Unit is largely reduced. In summary, this control structure is independent from the scale of the wind farm and suitable for modern wind farm control application.

The optimality of the D-MPC is dependent on the accuracy of the wind turbine model. The adopted model is a simplified model where some fast dynamics are ignored. In the practical operation, there exist errors and uncertainties in the system parameters, which include the inertias of the mechanical part, control parameters of pitch control and identified parameters. In this paper, in order to investigate the robustness of the D-MPC under parameter errors, the errors of the inertias and measurements are considered and the control parameters are assumed to be perfectly known. The errors existing in the inertias are assumed to be bounded and follow a normal distribution. The identified parameters rely on the measurements of state and input variables (effective wind speed estimation). Similarly, the measurement errors are also assumed to be bounded and follow a normal distribution. According to [22], linear systems with convex constraints have inherent robustness. The robustness of the developed method to errors and uncertainties is demonstrated in Section V.C.

V. CASE STUDIES

Case studies were conducted to test the efficacy of the developed D-MPC. Firstly, the convergence of the adopted fast dual gradient method is shown. The suitable maximum iteration number k_{max} was selected for the following simulation cases. Secondly, the operation of the wind farm under both low and high wind conditions was analyzed. The results of the conventional centralized control and C-MPC were compared with that of D-MPC. Thirdly, with the same settings as the second simulation, the errors of the system parameters were included to test the robustness of the D-MPC developed to errors and uncertainties. Fourthly, the dynamic performance of the D-MPC with a wind turbine disconnected and reconnected was simulated.

A wind farm comprised of 10×5 MW wind turbines was used as the test system. The sampling time of the wind farm control t_s was set as $1s$. The mean wind speed of each wind turbine was assumed to be known. All the wind turbines were in the derated operation. The wind field modeling considering turbulences and wake effects for the wind farm was generated from SimWindFarm [23], which is a toolbox for dynamic wind farm model, simulation and control. The prediction horizon for MPC was set as $n_p = 10$. The wind speed was considered as a measurable disturbance and the value for the prediction horizon is based on persistence assumption, suitable for the short period prediction.

A. Convergence with the fast dual gradient method

The convergence of the fast dual gradient with different $\mathbf{L}$ is illustrated in Fig. 2. The y-axis denotes the deviation to the constraints (see (7)). Apparently, the convergence rate with $\mathbf{L} \pm GH^{-1}G'$ is higher. Especially when $\mathbf{L} = GH^{-1}G'$, which has the tightest upper bounds, the convergence is fastest. Only 5 iterations can guarantee a good performance of the D-MPC. Therefore, the maximum iteration number is selected as $k_{max} = 5$ in this paper.
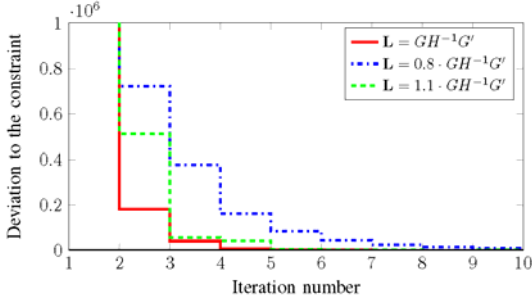
Fig. 2 Convergence comparison with different **L**

B. Operation under high and low wind conditions

The operation of the wind farm was simulated under both high and low wind conditions. Accordingly, the power references of the wind farm P_{ref}^{wfc} are defined as 40 MW and 30 MW and assumed to be constant during the simulation. For the wind input to individual wind turbines, the turbulence is assumed to be fixed. A constant difference (4m/s) is added in the mean part. As an example, the wind speed of WT 05 for both wind conditions is shown in Fig. 3, which covers the range between 11m/s and 20m/s . The mean values of all the wind turbines for both conditions are listed in Table II and IV, respectively. The simulation time is 300 s.
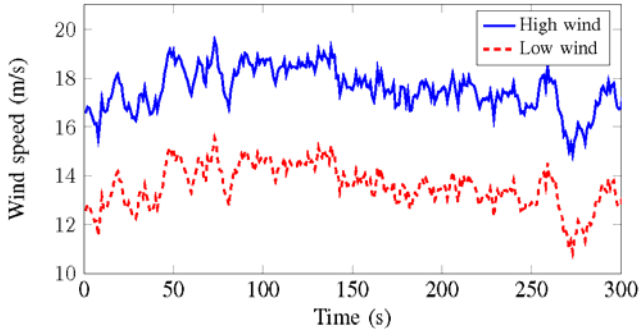

Fig. 3 Wind speed variation of WT 05

The weighting factors in the cost function (3) are defined as: $Q_P = 1$, $Q_T = 20$, $Q_F = 5$. As explained in [9], Q_F should be kept small to avoid violent control and shaft load increase.

For the centralized wind farm controller, the proportional distribution algorithm proposed in [4] is used. The power references for all the wind turbines are considered as the same. That means $P_{ref}^{WT_i} = \dfrac{P_{ref}^{wfc}}{n_t}$. For the high wind case, $P_{ref}^{WT_i}$ is 4 MW while $P_{ref}^{WF_i}$ is 3 MW for the low wind case.

1) Power reference tracking: To evaluate the primary objective of the wind farm controller, the comparison of P_{gen}^{wfc} for different controllers under both wind conditions is shown in Fig. 4.

The standard deviation $\sigma(P_{gen}^{wfc})$ is used to quantify the deviation to the references (40 MW in Fig. 4(a) and 30 MW in Fig. 4(b)), listed in Table I. It can be observed that the D-MPC shows almost identical control performance as the other two

controllers. For the high wind condition, all the controllers have the same standard deviation value (0.0081 MW), only 0.020% of the reference (40 MW). For the low wind condition, the standard deviations of the C-MPC and the D-MPC are same (0.0056 MW) and a bit smaller than that of the centralized controller (0.0057 MW). Compared with the reference value (30 MW), this tiny difference can be neglected.
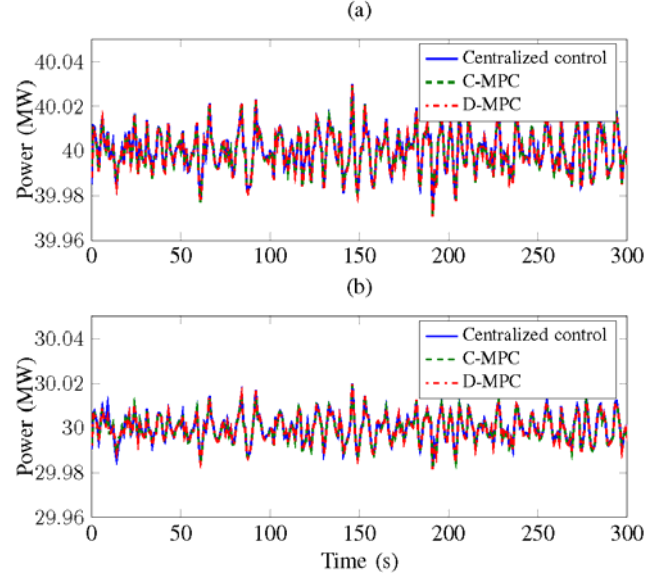

Fig. 4 Active power of the wind farm P_{gen}^{wfc} , (a) represents the high wind condition; (b) represents the low wind condition.

TABLE I
SIMULATION STATISTICS $\sigma(P_{gen}^{wfc})$ in MW

Wind Condition	Centralized Control	C-MPC	D-MPC
High Wind	0.0080	0.0080 (0.00%)	0.0080 (0.00%)
Low Wind	0.0057	0.0056 (-1.75%)	0.0056 (-1.75%)

2) Wind turbine load alleviation: The standard deviation $\sigma(T_s)$ and $\sigma(\Delta F_t)$ indicate the shaft and thrust-induced loads, respectively. The simulation results are listed in Table II-V to quantify the variation of the results of all wind turbines. According to the results in Table II and IV, the shaft torque deviation is largely reduced with the D-MPC for each wind turbine, compared with the centralized control. For the high wind case, the values range from 41.87% to 56.69% (Table II). For the low wind case, the reduction percentages of the standard deviation are between 34.98% and 55.45% (Table IV).

The thrust force change is also reduced to some extent in each wind turbine with the D-MPC, according to Table III and V. For the high wind case, the reduction percentages of standard deviation are between 0.00% and 2.81% (Table III). For the low wind case, the values are between 0.00% and 24.6% (Table V).

TABLE II
SIMULATION STATISTICS $\sigma(T_s)$ in 0.01MNm

Turbine	v_avr (m/s)	Centralized Control	C-MPC High Wind	D-MPC High Wind
WT 01	17.50	6.52	3.79 (-41.87%)	3.79 (-41.87%)
WT 02	17.02	6.99	3.33 (-52.36%)	3.33 (-52.36%)
WT 03	16.54	6.65	2.88 (-56.69%)	2.88 (-56.69%)
WT 04	16.64	6.48	3.22 (-50.31%)	3.22 (-50.31%)
WT 05	17.46	5.80	2.95 (-49.14%)	2.95 (-49.14%)
WT 06	17.00	5.70	3.10 (-45.61%)	3.10 (-45.61%)
WT 07	16.38	6.32	3.25 (-48.58%)	3.25 (-48.58%)
WT 08	17.14	6.11	2.84 (-53.52%)	2.84 (-53.52%)
WT 09	17.11	6.42	3.33 (-48.13%)	3.33 (-48.13%)
WT 10	16.45	7.26	3.70 (-49.04%)	3.70 (-49.04%)

TABLE III
SIMULATION STATISTICS $\sigma(\Delta F_t)$ in 0.01MN

Turbine	v_avr (m/s)	Centralized Control	C-MPC High Wind	D-MPC High Wind
WT 01	17.50	1.76	1.76 (-0.00%)	1.76 (-0.00%)
WT 02	17.02	1.93	1.89 (-2.07%)	1.89 (-2.07%)
WT 03	16.54	1.77	1.74 (-1.69%)	1.74 (-1.69%)
WT 04	16.64	1.78	1.72 (-3.37%)	1.72 (-3.37%)
WT 05	17.46	1.56	1.53 (-1.92%)	1.53 (-1.92%)
WT 06	17.00	1.66	1.64 (-1.20%)	1.64 (-1.20%)
WT 07	16.38	1.82	1.77 (-2.75%)	1.77 (-2.75%)
WT 08	17.14	1.76	1.74 (-1.14%)	1.74 (-1.14%)
WT 09	17.11	1.57	1.52 (-3.18%)	1.52 (-3.18%)
WT 10	16.45	1.99	1.94 (-2.51%)	1.94 (-2.51%)

TABLE IV
SIMULATION STATISTICS $\sigma(T_s)$ in 0.01MNm

Turbine	v_avr (m/s)	Centralized Control	C-MPC Low Wind	D-MPC Low Wind
WT 01	13.50	5.48	2.85 (-47.99%)	2.85 (-47.99%)
WT 02	13.02	5.78	2.71 (-53.11%)	2.71 (-53.11%)
WT 03	12.54	5.60	2.99 (-46.61%)	2.99 (-46.61%)
WT 04	12.64	6.06	3.94 (-34.98%)	3.94 (-34.98%)
WT 05	13.46	4.85	2.24 (-53.81%)	2.24 (-53.81%)
WT 06	13.00	4.77	2.22 (-53.46%)	2.22 (-53.46%)
WT 07	12.38	5.99	3.10 (-48.25%)	3.10 (-48.25%)
WT 08	13.14	5.05	2.25 (-55.45%)	2.25 (-55.45%)
WT 09	13.11	5.31	3.19 (-39.92%)	3.19 (-39.92%)
WT 10	12.45	6.69	3.91 (-41.55%)	3.91 (-41.55%)

Since the results of all wind turbines are similar, T_s and F_t of a single wind turbine (WT 05) with different controllers are illustrated in Fig. 5 and Fig. 6. It can be observed that the power reference by the MPC (C-MPC and D-MPC) varies following the wind speed (Fig. 5(a) and Fig. 6(a)). Accordingly, the deviation of the shaft torque T_s is

significantly reduced (Fig. 5(b) and Fig. 6(b)). The alleviation of the thrust force is not very obvious (Fig. 5(c) and Fig. 6(c)). Besides, the results show that the control inputs of both C-MPC and D-MPC are almost identical, which proves that the D-MPC has the same control performance as the C-MPC.

TABLE V
SIMULATION STATISTICS $\sigma(\Delta F_t)$ in 0.01MN

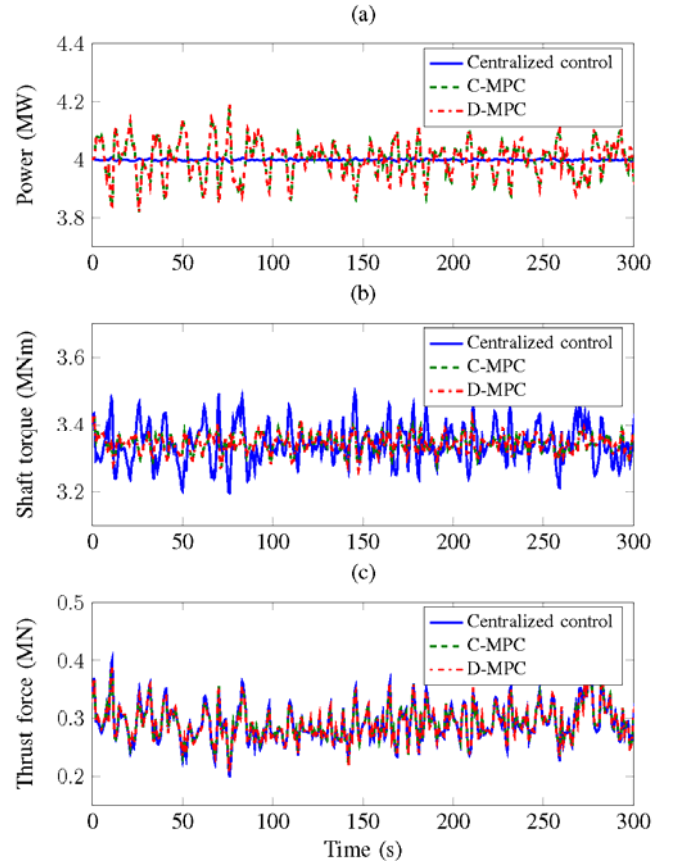| Turbine	v_avr (m/s)	Centralized Control	C-MPC Low Wind	D-MPC Low Wind
WT 01	13.50	1.85	1.84 (-0.54%)	1.84 (-0.54%)
WT 02	13.02	2.03	1.99 (-2.01%)	1.99 (-2.01%)
WT 03	12.54	1.92	1.85 (-3.65%)	1.85 (-3.65%)
WT 04	12.64	2.59	2.55 (-1.54%)	2.55 (-1.54%)
WT 05	13.46	1.63	1.59 (-2.45%)	1.59 (-2.45%)
WT 06	13.00	1.75	1.72 (-1.71%)	1.72 (-1.71%)
WT 07	12.38	2.64	1.95 (-26.1%)	1.95 (-26.1%)
WT 08	13.14	1.84	1.81 (-1.63%)	1.81 (-1.63%)
WT 09	13.11	1.72	1.65 (-4.02%)	1.65 (-4.02%)
WT 10	12.45	2.63	2.62 (-0.38%)	2.62 (-0.38%)

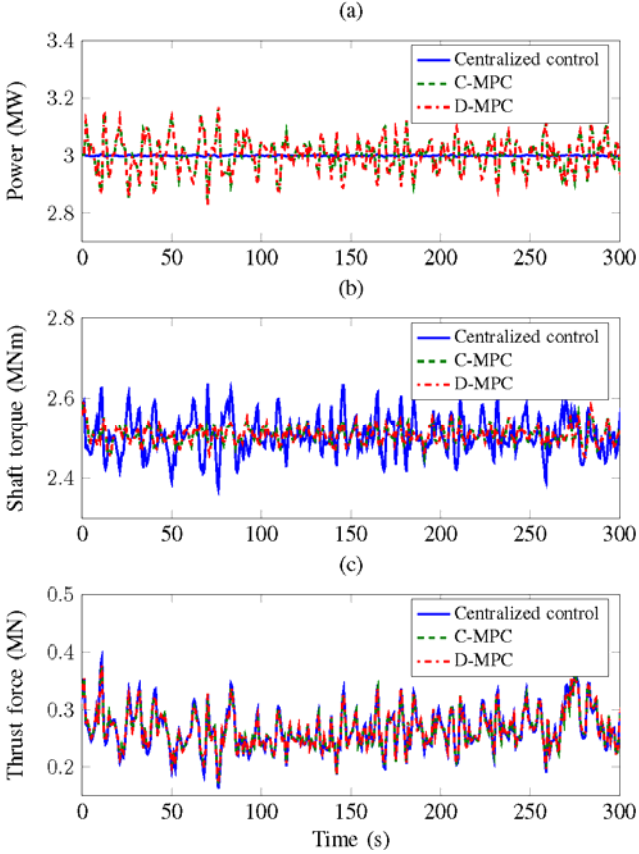Fig. 5 Simulation results of WT 05 under the high wind condition

Fig. 6 Simulation results of WT05 under the low wind condition

C. Robustness of D-MPC

In order to test the robustness of the developed D-MPC to errors and uncertainties, the errors existed in the inertias, the effective wind speed estimation and the state measurements were included. These errors are considered to follow the normal distribution $N(0, 0.1^2)$. The simulation settings are same as Section V.B. The control performances between D-MPC with and without errors were compared.

1) Power reference tracking: The comparison of $\sigma(P_{\text{gen}}^{\text{wfc}})$ for different D-MPCs under both wind conditions is listed in Table VI. The result of centralized control is taken as the reference.

TABLE VI
SIMULATION STATISTICS $\sigma(P_{\text{gen}}^{\text{wfc}})$ in MW

Wind Condition	D-MPC no error	D-MPC with error
High Wind	0.0080 (0.00%)	0.0081 (1.25%)
Low Wind	0.0056 (-1.75%)	0.0058 (1.75%)

For the high wind condition, it can be observed that the standard deviations of the D-MPC with errors is only a little bit larger than that of the D-MPC without errors (0.0080 MW), only 0.02% of the reference (40 MW). Similarly, for the low wind condition, the standard deviation of the D-MPC with errors is a little bit larger than that of D-MPC without errors

(0.0056 MW). Compared with the reference value (30 MW), this tiny difference can be neglected.

2) Wind turbine load alleviation: The comparisons of standard deviation $\sigma(T_s)$ and $\sigma(\Delta F_t)$ of all wind turbines for different D-MPCs under high and low wind conditions are listed in Tables VII-VIII, respectively. The result of the centralized control is taken as the reference.

TABLE VII
SIMULATION STATISTICS UNDER HIGH WIND

Turbine	$\sigma(T_s)$ in 0.01MNm		$\sigma(\Delta F_t)$ in 0.01MN	
	D-MPC no error	D-MPC with error	D-MPC no error	D-MPC with error
WT 01	3.79 (-41.87%)	4.10 (-37.12%)	1.76 (-0.00%)	1.76 (-0.00%)
WT 02	3.33 (-52.36%)	3.70 (-47.07%)	1.89 (-2.07%)	1.90 (-1.55%)
WT 03	2.88 (-56.69%)	3.09 (-53.53%)	1.74 (-1.69%)	1.73 (-2.26%)
WT 04	3.22 (-50.31%)	3.59 (-44.60%)	1.72 (-3.37%)	1.73 (-2.81%)
WT 05	2.95 (-49.14%)	3.30 (-43.10%)	1.53 (-1.92%)	1.54 (-1.28%)
WT 06	3.10 (-45.61%)	3.46 (-39.30%)	1.64 (-1.20%)	1.64 (-1.20%)
WT 07	3.25 (-48.58%)	3.46 (-45.25%)	1.77 (-2.75%)	1.80 (-1.10%)
WT 08	2.84 (-53.52%)	3.24 (-46.97%)	1.74 (-1.14%)	1.75 (-0.57%)
WT 09	3.33 (-48.13%)	3.66 (-42.99%)	1.52 (-3.18%)	1.54 (-1.91%)
WT 10	3.70 (-49.04%)	4.05 (-44.21%)	1.94 (-2.51%)	1.96 (-1.51%)

TABLE VIII
SIMULATION STATISTICS UNDER LOW WIND

Turbine	$\sigma(T_s)$ in 0.01MNm		$\sigma(\Delta F_t)$ in 0.01MN	
	D-MPC no error	D-MPC with error	D-MPC no error	D-MPC with error
WT 01	2.85 (-47.99%)	3.06 (-44.16%)	1.84 (-0.54%)	1.85 (-0.00%)
WT 02	2.71 (-53.11%)	3.02 (-47.75%)	1.99 (-2.01%)	2.00 (-1.48%)
WT 03	2.99 (-46.61%)	3.35 (-40.18%)	1.85 (-3.65%)	1.85 (-3.65%)
WT 04	3.94 (-34.98%)	4.29 (-29.21%)	2.55 (-1.54%)	2.54 (-1.93%)
WT 05	2.24 (-53.81%)	2.44 (-49.69%)	1.59 (-2.45%)	1.61 (-1.23%)
WT 06	2.22 (-53.46%)	2.53 (-46.96%)	1.72 (-1.71%)	1.72 (-1.71%)
WT 07	3.10 (-48.25%)	3.16 (-47.25%)	1.95 (-26.1%)	1.99 (-24.6%)
WT 08	2.25 (-55.45%)	2.52 (-50.10%)	1.81 (-1.63%)	1.81 (-1.63%)
WT 09	3.19 (-39.92%)	3.20 (-39.74%)	1.65 (-4.07%)	1.67 (-2.91%)
WT 10	3.91 (-41.55%)	3.98 (-40.51%)	2.62 (-0.38%)	2.62 (-0.38%)

For $\sigma(T_s)$, with the existence of errors, the reduction percentages are from 37.12% to 53.53% for the high wind case (Table VII) and from 29.21% to 50.10% for the low wind case (Table VIII). Compared with the results without errors, the shaft torque deviations increase slightly for each turbine. Although the control performance becomes a little bit worse, the shaft torque deviation is still largely reduced.

For $\sigma(\Delta F_t)$, with the existence of errors, the reduction percentages are from 0.00% to 2.81% for the high wind case (Table VII) and from 0.00% to 24.6% for the low wind case (Table VIII). Similarly, the control performance becomes a little bit worse. However, the thrust force is still alleviated to some extent.

D. Disconnection and Reconnection of a wind turbine

In the wind farm operation, it is common that a certain wind turbine is disconnected or reconnected. In this part, the dynamic performance of the D-MPC is simulated with a certain wind turbine disconnected and reconnected to show the

control flexibility. In order to illustrate the results, it is assumed that only 4 turbines (WT 01-WT 04) are in operation. The simulation time is set 300 s. The simulation events are as follows: At $t = 100s$ WT 03 is disconnected; At $t = 200s$, WT 03 is reconnected. Accordingly, the wind farm reference is set as follows: during $0s \sim 100s$, $P_{ref}^{wfc} = 16MW$; During $100s \sim 200s$, WT 03 is detected to be out of service and P_{ref}^{wfc} decreases to $12MW$; During $200s \sim 300s$, WT 03 is reconnected and P_{ref}^{wfc} goes back to $16MW$.

The simulation results are illustrated in Fig. 7, including the power references derived by the D-MPC $P_{ref}^{WT_i}$ (Fig. 7(a)) and total output power P_{gen}^{wfc} (Fig. 7(b)). When WT 03 is out of service ($100s \sim 200s$), the "mean power reference generation" block (see Fig. 1) will redistribute the mean references to the other turbines. In this case, the mean references are maintained: $\overline{P_{ref}^{WT_i}} = 4MW$ ($i = 1, 2, 4.$). As aforementioned, the corresponding $\mathbf{L}_i^{-1}$ ($i = 3$) is set 0 and it is not involved in the $\mathbf{L}^{-1}$ formulation at each sampling point according to (18). The rest D-MPC controllers ($i = 1, 2, 4.$) are coordinated to track the new power reference of the wind farm $P_{ref}^{wfc} = 12MW$ as well as minimize the mechanical loads of the rest wind turbines. A good tracking performance can be observed in Fig. 7(b).
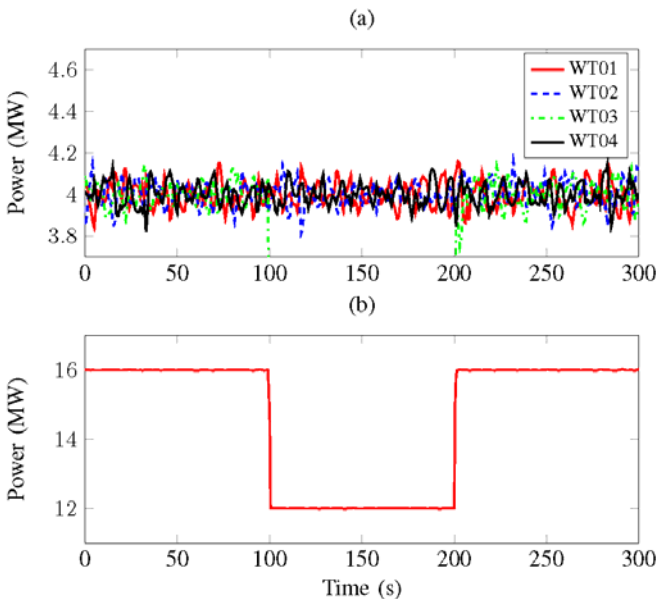

Fig. 7 Simulation results when WT03 is out of service during 100s-200s

VI. CONCLUSION

In this paper, the D-MPC algorithm based on the fast dual gradient method is developed for the active power control of a wind farm. Compared with the conventional wind farm control, the D-MPC strikes a balance between the power reference tracking and the minimization of the wind turbine loads. Different from C-MPC, in the developed D-MPC, most of computation tasks are distributed to the local D-MPCs equipped at each wind turbine. The computation burden of the central unit is significantly reduced which is only responsible for the update of dual variables. This control structure is independent from the scale of the wind farm. Besides, with properly calculated Lipschitz constant $\mathbf{L}$, the adopted fast dual gradient method can significantly improve the convergence rate from $O(1/k)$ to $O(1/k^2)$, which reduces the iteration number. Consequently, the communication burden between local D-MPC and central unit is largely reduced. By means of the developed PWA model in Part I, the calculation work of $\mathbf{L}$ dependent on the model parameter of the operation region can be done off-line and stored. Through different case studies, the power tracking control performances of the developed D-MPC are verified to be identical to these of C-MPC. The mechanical loads experienced by individual wind turbines have been largely alleviated without affecting tracking the power reference of the wind farm. The robustness of D-MPC to errors and uncertainties of system parameters is also investigated and verified by including errors of the mechanical inertias and measurements. The D-MPC can be used for real-time control of modern wind farms.

REFERENCES

[1] I. Erlich and U. Bachmann, "Grid code requirements concerning connection and operation of wind turbines in Germany," in *Proc. 2005 IEEE Power Engineering Society General Meeting*, pp. 1253–1257.

[2] I. Erlich, W. Winter, and A. Dittrich, "Advanced grid requirements for the integration of wind turbines into the German transmission system," in *Proc. 2006 IEEE Power Engineering Society General Meeting*, pp. 7–pp. 14.

[3] M. Tsili and S. Papathanassiou, "A review of grid code technical requirements for wind farms," *IET Renew. Power Gen.*, vol. 3, no. 3, pp. 308–332, 2009.

[4] P. E. Sørensen, A. D. Hansen, F. Iov, F. Blaabjerg, and M. H. Donovan, "Wind farm models and control strategies," Risø National Laboratory, Tech. Rep., Risø-4-1464, Aug. 2005.

[5] Z. Lubosny and J. W. Bialek, "Supervisory control of a wind farm," *IEEE Trans. on Power Syst.*, vol. 22, no. 3, pp. 985–994, 2007.

[6] I. Munteanu, A.I. Bratcu, N.A. Cutululis, et al, *Optimal control of wind energy systems: towards a global approach*. Springer, 2008.

[7] B. Biegel, D. Madjidian, V. Spudic, A. Rantzer, and J. Stoustrup, "Distributed low-complexity controller for wind power plant in derated operation," in *Proc. 2013 IEEE International Conf. on Control Applications (CCA)*, pp. 146–151.

[8] D. Madjidian, K. Martensson, and A. Rantzer, "A distributed power coordination scheme for fatigue load reduction in wind farms," in *Proc. 2011 IEEE American Control Conf. (ACC)*, pp. 5219–5224.

[9] V. Spudić, M. Jelavić, and M. Baotić, "Wind turbine power references in coordinated control of wind farms," *Automatika–Journal for Control, Measurement, Electronics, Computing and Communications*, vol. 52, no. 2, 2011.

[10] V. Spudić, M. Jelavić, M. Baotić, and N. Perić, "Hierarchical wind farm control for power/load optimization," in *Proc. 2010 The Science of making Torque from Wind (Torque2010)*.

[11] S. Teleke, M. Baran, S. Bhattacharya, and A. Huang, "Rule-based control of battery energy storage for dispatching intermittent renewable sources," *IEEE Trans. Sustain. Energy*, vol. 1, no. 3, pp. 117–124, 2010.

[12] B. T. Stewart, A. N. Venkat, J. B. Rawlings, S. J. Wright, and G. Pannocchia, "Cooperative distributed model predictive control," *Systems & Control Letters*, vol. 59, no. 8, pp. 460–469, 2010.

[13] M. D. Doan, T. Keviczky, and B. De Schutter, "An improved distributed version of han's method for distributed MPC of canal systems," in *Symposium on Large Scale Systems: Theory and Applications*, 2010.

[14] H. Everett III, "Generalized Lagrange multiplier method for solving problems of optimum allocation of resources," *Operations research*, vol. 11, no. 3, pp. 399–417, 1963.

[15] M. D. Doan, T. Keviczky, and B. De Schutter, "An iterative scheme for distributed model predictive control using fenchel's duality," *Journal of Process Control*, vol. 21, no. 5, pp. 746–755, 2011.

[16] P. Giselsson, M. D. Doan, T. Keviczky, B. D. Schutter, and A. Rantzer, "Accelerated gradient methods and dual decomposition in distributed model predictive control," *Automatica*, vol. 49, no. 3, pp. 829–833, 2013.

[17] P. Giselsson, "Improving fast dual ascent for MPC-Part I: The distributed case, " *arXiv preprint arXiv:1312.3012,* 2013.

[18] P. Giselsson, "Improving fast dual ascent for MPC-Part II: The embedded case," *arXiv preprint arXiv:1312.3013,* 2013.

[19] T. Burton, N. Jenkins, D. Sharpe, and E. Bossanyi, *Wind energy handbook*. John Wiley & Sons, 2011.

[20] M. N. Soltani, T. Kundsen, M. Svenstrup, R. Wisniewski, P. Brath, R. Ortega, "Estimation of rotor effective wind speed: A comparison," *IEEE Trans. Control Syst. Technol.*, vol. 21, no. 4, pp. 1155-1167, 2013.

[21] J. M. Maciejowski, *Predictive control: with constraints.* Pearson education, 2002.

[22] G. Grimm, M. J. Messina, S. E. Tuna and A. R. Teel, "Examples when nonlinear model predictive control is nonrobust," *Automatica*, vol.40, no. 10, pp. 1729-1738, 2004

[23] J. D. Grunnet, M. Soltani, T. Knudsen, M. Kragelund, and T. Bak, "Aeolus toolbox for dynamic wind farm model, simulation and control," in *Proc. 2010 European Wind Energy Conference&Exhibition*, 2010.